BIOMASS: ESA's P-Band SAR Mission

Citation for the original published paper (version of record):

Scipal, K., Albinet, C., Caccia, M. et al (2026). BIOMASS: ESA's P-Band SAR Mission. Proceedings of the IEEE, 114(2): 220-235. http://dx.doi.org/10.1109/JPROC.2026.3687416

(article starts on next page)

INVITED PAPER

BIOMASS: ESA's P-Band SAR Mission

This article describes the pre-launch status of ESA's BIOMASS mission, the first P-band SAR system to be operated from Earth orbit.

By Klaus Scipal, *Member IEEE*, Clément Albinet, Michele Caccia, Adriano Carbone, Nuno Carvalhais, Jérôme Chave, Jørgen Dall, *Member IEEE*, Michael Fehringer, Antonio Leanza, Thuy Le Toan, Maktar Malik, Antonio Novelli, Philippe Paillou, Kostas P. Papathanassiou, *Fellow IEEE*, Janice Patterson, Muriel Pinheiro, Shaun Quegan, Markus Reichstein, Björn Rommen, Sassan Saatchi, Herman H. Shugart, Tristan Simon, Stefano Tebaldini, *Senior Member IEEE*, Lars M. H. Ulander, *Fellow IEEE*, Antonio Valentino, Philip Willemsen, and Mathew Williams

ABSTRACT | The European Space Agency's (ESA) BIOMASS mission is a pioneering Earth observation satellite mission launched on April 29, 2025. Utilizing a P-band synthetic aperture radar (SAR), the objective of BIOMASS is to deliver estimates of above-ground forest biomass, forest height (FH), and forest disturbance (FD), with unprecedented accuracy. The mission's primary scientific goal is to quantify the distribution and changes in forest biomass, thereby reducing uncertainties in carbon flux estimates and informing climate models. The satellite's advanced instrumentation and innovative approach allow it to penetrate dense forest canopies, capturing data even in challenging environments. The mission will operate in two distinct phases: the tomographic phase and the interferometric phase, which will support polarimetric interferometric SAR (Pol-InSAR) and tomographic SAR (TomoSAR) processing. Additionally, BIOMASS will provide valuable observational data for ice sheets, deserts, the ionosphere, below canopy topography, and other domains.

KEYWORDS | BIOMASS; carbon cycle; P band; SAR polarimetry; SAR tomography; satellite; synthetic aperture radar (SAR) interferometry.

Received 1 April 2025; revised 26 February 2026; accepted 6 April 2026. Date of publication 15 May 2026; date of current version 14 July 2026. *(Corresponding author: Klaus Scipal.)*

Klaus Scipal, **Clément Albinet**, and **Muriel Pinheiro** are with European Space Research Institute, European Space Agency, 00044 Frascati, Italy (e-mail: Klaus.Scipal@esa.int).

Michele Caccia, **Antonio Novelli**, and **Antonio Valentino** are with Starion Italia s.p., 00044 Frascati, Italy.

Adriano Carbone, **Michael Fehringer**, **Antonio Leanza**, **Maktar Malik**, **Janice Patterson**, **Björn Rommen**, **Tristan Simon**, and **Philip Willemsen** are with the Space Research and Technology Centre, 2210 AZ Noordwijk, The Netherlands.

Nuno Carvalhais is with the Max Planck Institute for Biogeochemistry, 07745 Jena, Germany, with the Departamento de Ciências e Engenharia do Ambiente (DCEA), Faculdade de Ciências e Tecnologia (FCT), Universidade Nova de Lisboa, 2829-516 Caparica, Portugal, and also with the ELLIS Unit Jena, 07745 Jena, Germany.

Jérôme Chave is with CNRS, Laboratoire Evolution et Diversité Biologique, Université Paul Sabatier, 5174 Toulouse, France.

Jørgen Dall is with the Technical University of Denmark, 2800 Kongens Lyngby, Denmark.

Thuy Le Toan is with the Centre d'Etudes Spatiales de la Biosphère, 31400 Toulouse, France.

Philippe Paillou is with the University of Bordeaux, 33076 Bordeaux, France.

Kostas P. Papathanassiou is with German Aerospace Center, 82234 Weßling, Germany.

Shaun Quegan is with the University of Sheffield, S10 2TN Sheffield, U.K., and also with the National Centre for Earth Observation, LE4 5SP Leicester, U.K.

Markus Reichstein is with the Max Planck Institute for Biogeochemistry, 07745 Jena, Germany.

Sassan Saatchi is with the Jet Propulsion Laboratory, Pasadena, CA 91109 USA.

Herman H. Shugart is with the University of Virginia, Charlottesville, VA 22904 USA.

Stefano Tebaldini is with the Department of Electronics, Information, and Bioengineering, Politecnico di Milano, 20133 Milan, Italy.

Lars M. H. Ulander is with the Chalmers University of Technology, 412 96 Gothenburg, Sweden.

Mathew Williams is with the School of Geosciences, The University of Edinburgh, EH9 3FF Edinburgh, U.K.

Digital Object Identifier 10.1109/JPROC.2026.3687416

I. INTRODUCTION

European Space Agency's (ESA) Earth Explorer missions are a cornerstone of its FutureEO program, designed to address critical scientific questions about the Earth system. This program focuses on understanding the complex interactions between the atmosphere, biosphere, hydrosphere, cryosphere, and lithosphere, providing essential data for climate research and environmental monitoring [1]. The most recently launched mission under this program is BIOMASS, which aims to quantify forest carbon stocks and changes globally by measuring above-ground forest biomass and forest height (FH).

Forests play a crucial role in the global carbon cycle and the climate system. They hold significant carbon stocks and act as dominant sinks, absorbing carbon dioxide (CO_2) from the atmosphere through net primary production and storing it in biomass and soil. Forests can also be substantial carbon sources, releasing CO_2 to the atmosphere through natural disturbance events, such as wildfire, pests, or drought-induced mortality, but also through deforestation and degradation processes from anthropogenic activities.

The development of carbon sinks, known as carbon sequestration, helps mitigate climate change by reducing the concentration of greenhouse gases in the atmosphere [2], [3]. The carbon sequestration capacity of forests is immense, holding approximately 70% of total ecosystem carbon on land, and varies globally, influenced inter alia by forest age, health, species composition, hydrometeorology, topography, soil composition, and climate. In particular, tropical moist forests hold the largest biomass carbon stocks on the planet. The importance of these forests calls for an enhanced understanding of their functioning and makes their conservation and sustainable management critical for climate change mitigation [4]. These forests face numerous threats that undermine their ability to sequester carbon and regulate the climate. Field sampling suggests that carbon sequestration rates have stayed stable in African tropical forests [5] but declined in Amazonian tropical forests [6]. Deforestation and forest degradation are among the most significant threats, driven by factors such as agricultural expansion, logging, and infrastructure development [7]. Besides human activities, climate change itself poses a significant threat. Increasing temperatures, altered precipitation patterns, extreme weather events, insect infestations, and fires can all degrade forest ecosystems with negative impacts on forest health, growth, and their future carbon sequestration capacity [8], [9], [10], [11]. According to [12], around 10% of the annual anthropogenic emissions of CO_2 to the atmosphere are from land use change, making deforestation processes a major carbon emitter, second only to fossil fuel emissions, though the relative uncertainty in this value is large at $\sim$65%, as degradation and regrowth dynamics are poorly quantified. Due to the widespread deforestation and disturbance in tropical forests, boreal forests have the potential to become a more important sink than tropical forests [13], [14] but, like tropical forests, their ability to sequester carbon is increasingly affected by degradation and deforestation [15], [16]. Understanding the drivers of deforestation, forest degradation, and forest disturbance (FD) and how they affect forest ecosystems, including the physiological responses of trees to climate stressors, changes in atmospheric CO_2, and the potential for forests to adapt to changing conditions [17], is therefore essential for understanding forests' role in the global carbon cycle and how their capacity to store carbon will change in future.

Beyond their central role in the global carbon cycle, forests also influence local and global climates by regulating the water cycle, the Earth's radiative energy balance, and cloud formation [2], [18]. They provide a wide range of essential ecosystem services, including the interception of water, mitigating floods, the filtration of water, the stabilization of soils, the supply of building materials and fuelwood, and the provision of key habitats for wildlife [18]. They also hold significant cultural value and contribute to human wellbeing.

Given their importance, understanding how forests function—and how they are changing—has become increasingly urgent. Although forests are fundamental to the climate system and provide vital ecosystem services, major research challenges remain in assessing the influence of human activities and climate change on forest dynamics. Land use change and terrestrial CO_2 uptake—reflecting losses and gains of forest biomass—continue to present some of the largest uncertainties in the global carbon budget [12]. While our qualitative understanding of forest processes is well developed, major gaps persist in their quantitative assessment, making the study of forest ecosystem dynamics an urgent scientific priority.

Accurately estimating the carbon stored in forests is a major challenge. Typically, the carbon stored in trees is derived from an estimate of the above-ground forest biomass, which in turn is derived from forest structural measurements. Forest ecosystems are highly complex, with carbon storage and release influenced by many factors, including stand structure, forest age, species composition, soil type, disturbance, and management practices [3]. Thus, for monitoring, it is important to characterize forests not only by a single number (e.g., leaf area index or biomass) but also to embrace structural information such as the vertical distribution of biomass.

Traditional methods to measure forest structure and estimate biomass, such as forest inventories, have limitations in terms of coverage and repeatability. Modern sensor technology such as airborne lidar scanning [19] and drone lidar [20] or terrestrial lidar scanning [21], [22] can complement ground-based forest census observations, capturing forest structural information on a landscape scale up to several square kilometers or providing accurate 3-D forest structure models. However, these technologies cannot provide the required wide area mapping capabilities needed, for instance, in the pan-tropics. Satellite imagery has the potential to overcome these limitations and offer new opportunities to improve the accuracy of biomass estimation [4]. In particular, synthetic aperture radars (SARs) [23], spaceborne lidar [24], and low-frequency passive microwave instruments [25] have been used individually or in various combinations to produce global biomass maps. Building on these advances, the ESA CCI Biomass time series provides annual global above-ground biomass maps at 100-m resolution for 2007–2022, calibrated using extensive LiDAR measurements from NASA's GEDI and ICESat-2 missions to improve allometries and temporal consistency [26]. Another example of a pantropical biomass dataset has been created through the fusion of GEDI lidar with TanDEM-X SAR, delivering 25- and 100-m resolution above-ground biomass maps for regions, including the Amazon Basin, Gabon, French Guiana, and Mexico, offering high-detail wall-to-wall estimates in tropical forests [27]. Complementing these global products are a range of regional and local products. While these products are widely used today, they usually do not meet the full array of requirements expressed by the scientific community, due to lacks in resolution, revisit, or sensitivity to forest structure in dense forest environments.

The BIOMASS satellite, launched on April 29, 2025, is designed to address these scientific challenges by providing repeated, spatially continuous low-frequency (P band, 432–438 MHz) SAR measurements. Low-frequency SAR can penetrate deep into the densest forest canopies and, in combination with novel information retrieval concepts such as polarimetric interferometric SAR (Pol-InSAR) [28], [29], [30] and tomographic SAR (TomoSAR) [31], [32], [33], can map forest structure parameters such as above-ground forest biomass density (AGBD) and FH with accuracies in the range of 20%–30%, which is comparable to ground-based observations [34], [35].

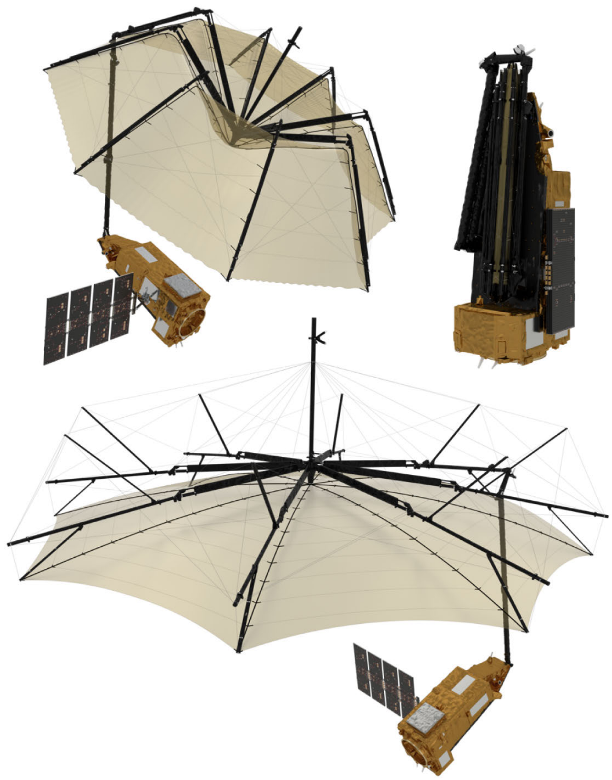

Fig. 1. ***Graphical sketch of the BIOMASS satellite in stowed, unfolding, and deployed configuration.***

II. MISSION OBJECTIVES

The primary scientific goal of the BIOMASS mission is to reduce the major uncertainties in calculations of carbon stocks and fluxes associated with the terrestrial biosphere, including those related to land use change, forest degradation, and forest regrowth. To achieve this goal, the primary objective of the BIOMASS mission is to deliver estimates of AGBD, FH, and FD, all of which are crucial for understanding forest structure and dynamics. To fulfill the scientific community's demand for accurate and comprehensive forest data, the mission's products must meet the following high-level requirements.

1) *Ability to Map Tropical Dense Forests:* The measurement system must be capable of accurately estimating biomass in tropical regions, where the combined effect of deforestation, forest degradation, and forest regrowth makes a major contribution to global land use emissions [7]. These regions are critical due to their significant carbon fluxes, yet are where we have the least information and knowledge [36].

2) *Hectare-Scale Estimates:* Estimates of AGBD, FH, and FD need to be available at a resolution around a hectare, which is the effective scale of forest variability [37]. This fine-scale resolution, particularly in conjunction with the vertical distribution of tree mass, can capture localized changes in forest biomass such as the falling of large canopy trees and the subsequent gap filling.

3) *Wall-to-Wall Coverage With Repeated Measurements:* Due to the diversity and fragmentation of tropical forests, the mission must provide spatially continuous coverage of tropical and subtropical forested regions with repeated measurements over multiple years, enabling the identification and monitoring of deforestation and regrowth patterns over time [35], [38], [39].

4) *Target Accuracy:* The target accuracy for AGBD and FH products is 20% at 4-ha resolution, comparable to ground-based observations. Achieving this level of accuracy is crucial for ensuring the reliability of satellite data for scientific research and policymaking [40], [41].

These high-level objectives have been used to size and design the mission. Secondary applications to map ice, deserts, topography, and the ionosphere, taking full benefit of the novel BIOMASS P-band SAR observation capabilities, have also been identified but were not used to drive the mission design.

III. SATELLITE DESIGN

BIOMASS is implemented as a single-platform, P-band (435 MHz) fully polarimetric SAR with an orbit enabling repeat-pass interferometric processing of the data (Fig. 1).

A. Platform

The satellite platform comprises two major elements, the mechanical platform (structure, propulsion, solar array, and harness) and the avionics platform (command and data handling, power, comms., payload data handling and attitude, and orbit control system AOCS) [42]. For the mechanical platform, an aluminum composite panel, H-structure design, is used as the core structure, building on heritage from Mars Express, Venus Express, and Aeolus missions. This structural concept meets the mass, stiffness, and pointing stability requirements of the mission. A monopropellant, hydrazine propulsion system with a single tank and four pairs of thrusters is implemented to provide orbit maintenance delta-V and attitude control capability for rate damping during initial acquisition and safe modes. A single deployable fixed solar array featuring 7 m^2 of triple junction gallium arsenide (GaAs) cells generates 1.5 kW of power. which is stored in a 156-Ah lithium-ion battery, ensuring continuous operation even during periods of eclipse.

The avionics platform is based on the Airbus AS250 platform, which was also used on the Sentinel-5P mission and has been adapted to fulfill the BIOMASS requirements. It is three-axis stabilized with yaw steering, providing precise orientation control. To control the deployment of the large deployable reflector (LDR), a customized reflector deployment interface unit is implemented. The AOCS is also customized with higher capability reaction wheels, larger magnetorquers, and a GNSS receiver to be able to cope with the wide range of system inertias during the deployment. For telemetry and telecommand (TC/TM), the satellite utilizes an S-band communication system with a 64-kb/s uplink and a 571-kb/s downlink. The scientific data collected by the satellite are transmitted via an X-band communication system, which provides a high-speed downlink at 500 Mb/s, essential for the timely transmission of the large volumes of data generated by the SAR system.

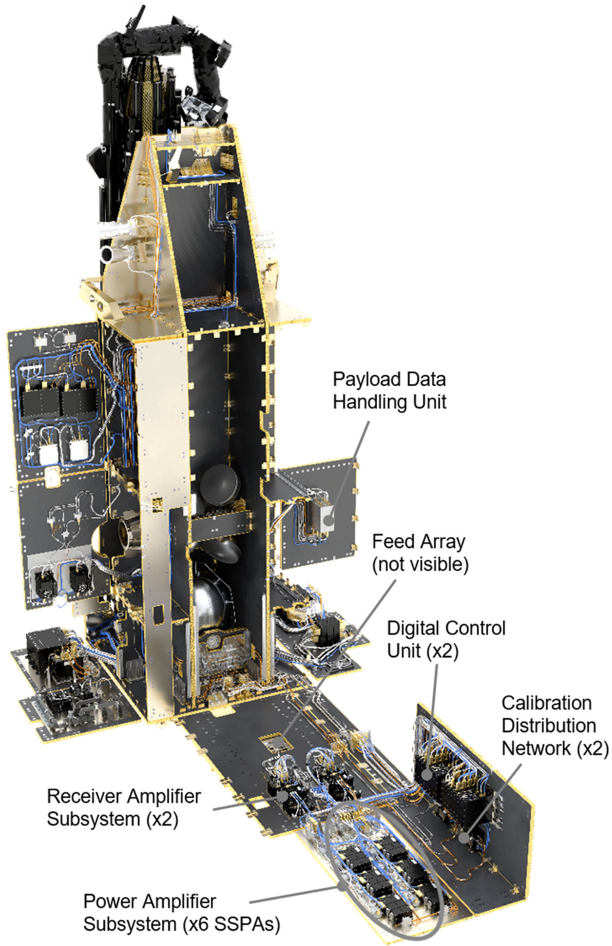

Fig. 2. *Image of the BIOMASS instrument and its integration on the platform.*

B. Instrument

The BIOMASS SAR instrument operates at 435 MHz with a 6-MHz bandwidth and with a fully polarimetric transmit and receive chain, capable of transmitting and receiving signals in H and V linear polarizations that allow the full polarimetric scattering matrix [43] to be measured. The comparatively small bandwidth of 6 MHz is in line with the frequency allocation to Earth Exploration Satellite Service in the 432–438-MHz band of the International Telecommunication Union (ITU) Radio Regulations. The most distinctive feature of the satellite is the LDR antenna with a projected circular aperture and diameter of approximately 12 m, a focal length of 7.8 m, and an offset of 2.1 m. The LDR was mounted on the side of the satellite platform and folded for launch so that it could be accommodated within the rocket fairing. On the outer side of the satellite at the bottom of the instrument panel, the antenna feed array (FA) is positioned, consisting of four patches connected to the instrument as two doublets (2×2). The main functions of the FA are the radio frequency (RF) signal transmission and reception for the BIOMASS SAR instrument. Each doublet consists of two patches, an FA network and two input ports, one per polarization.

On the inner side of the instrument panel, located in the platform interior, the instrument architecture consists of the following:

1) digital control unit (DCU);
2) calibration and distribution network (CDN);
3) power amplifier subsystem (PAS);
4) receive amplifier subsystem (RAS).

Fig. 2 provides an image of the Biomass instrument and platform.

The DCU is the heart of the instrument and performs the instrument control and internal calibration functions. The CDN routes the transmit RF signals generated by the DCU to the PAS and routes the received radar ground echo via the RAS back to the receive modules in the DCU. In addition, it ensures routing of the internal calibration signals through the instrument elements. The function of the PAS is to amplify the RF transmit chirp (Tx) to a peak power of +49.5 dBm (90 W) (adjustable by ± 1 dB). The PAS is composed of two identical assemblies, one for vertical and one

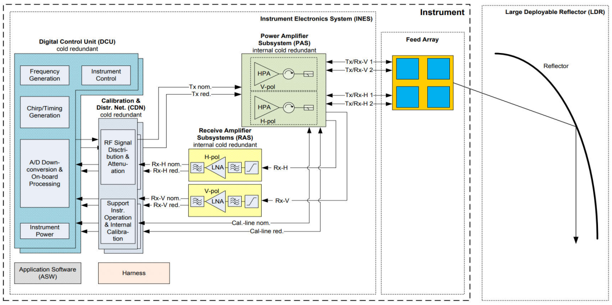

Fig. 3. ***Instrument block diagram [43], ©Airbus Germany.***

for horizontal polarization. Each PAS assembly contains two nominal solid-state power amplifiers (SSPAs), operating in parallel for power amplification of the Tx chirp, and one redundant SSPA. The main function of the RAS is to route and amplify the received radar echo from the PAS to the CDN at low noise (RAS noise figure < 2.3 dB) for each polarization. The DBIOMASS Instrument Proto Flight Model (PFM) contains two RAS: one for V and one for H polarization. Each unit is internally redundant (Fig. 3).

The latest available pre-flight instrument predicted performance values based on laboratory measurements and analysis performed as part of the satellite qualification review are given in Table 1 together with the confidence levels, applying to the acquisitions. Where a specific confidence level has not been specified, the performance level is considered as a worst case (w.c.) value. Parameters affected by the ionosphere (such as geolocation or residual phase error) assume no ionospheric impact. The pre-flight predicted performance is better than the requirements requested by the scientific community [44] except for the across-track peak-to-sidelobe ratio (PSLR), which is not compliant at the near edge of Swath 1, and the channel imbalance, which is not compliant at the required 3 sigma level. The requirement of the across-track PSLR is -16 dB, and the current noncompliance is not considered critical. The requirement of the channel imbalance is -25 dB and compliance is critical to achieve the polarimetric performance. The current approach to mitigate this noncompliance is to compensate the channel imbalance distortion using channel imbalance measurements over the BIOMASS Calibration Transponder (BCT) and over suitable distributed targets [45].

The first results obtained at the end of the commissioning phase indicate that all performance goals have been met and exceeded.

The instrument is operated in a stripmap left-looking imaging geometry. Platform rolls enable access to three swaths (Fig. 4). At the equator, for the ascending node, the incidence angle ranges per swath are 23.00°–27.79° for Swath 1, 27.06°–31.18° for Swath 2, and 30.49° to 33.90° for Swath 3. The resulting swath widths are 51.1 km for Swath 1, 54.5 km for Swath 2, and 52.0 km for Swath 3. The overlaps between Swaths 1 and 2, and between Swaths 2 and 3 are about 10 km. Incidence angles, swath widths, and swath overlaps vary slightly between ascending and descending orbits and with latitude and between mission phases.

C. Calibration

The BIOMASS mission gives completely new challenges in external calibration arising from the orbital pattern needed for the tomographic and Pol-InSAR phases of the mission, the strong effects of the ionosphere at P band, and the lack of preexisting P-band data. Together, these create problems that can only be solved by combining infrequent visits to instrumented calibration sites with systematic exploitation of the properties of distributed targets and targets of opportunity [43]. For system calibration, BIOMASS uses the active BCT transponder [46]. The BCT antenna is a 4.8-diameter 2-D array composed of 40 active patches

Table 1 Biomass System Requirements and Predicted Performance

Parameter	Requirement	Specification
Channel Imbalance	≤ -25 dB (3σ), Tx and Rx combined	≤ -23.5 dB (3σ), Tx and Rx combined
Cross-Talk	≤ -30 dB (3σ)	≤ -33.2 dB (3σ)
Radiometric bias	≤ 0.3 dB (1σ)	≤ 0.23 dB (1σ)
Radiometric stability	≤ 0.5 dB (1σ)	≤ 0.26 dB (1σ)
Noise Equivalent Sigma Nought	≤ -27 dB (w.c.)	≤ -30.4 dB (w.c.)
Total Ambiguity Ratio	≤ -18 dB (w.c.)	≤ -19.1 dB (w.c.)
Spatial resolution (SLC), range and azimuth	60 m x 8 m	59 m x 8 m
Residual phase error over pulse travel time	≤ 10 deg (1σ)	≤ 4.0 deg (1σ)
Residual phase error over data take time (12 min)	≤ 10 deg (1σ)	≤ 3.7 deg (1σ)
Peak to Sidelobe Ratio Along Track	≤ -16 dB (w.c.)	≤ -18.0 dB (w.c.)
Peak to Sidelobe Ratio Across Track	≤ -16 dB (w.c.)	≤ -14.1 dB (w.c.)
Integrated Sidelobe Ratio	≤ -9 dB (w.c.)	≤ -9.4 dB (w.c.)
Geo-location accuracy	≤ 25 m (w.c.)	≤ 4.1 m (w.c.)
Dynamic range	-30 dB to 5 dB	-30 dB to 5 dB

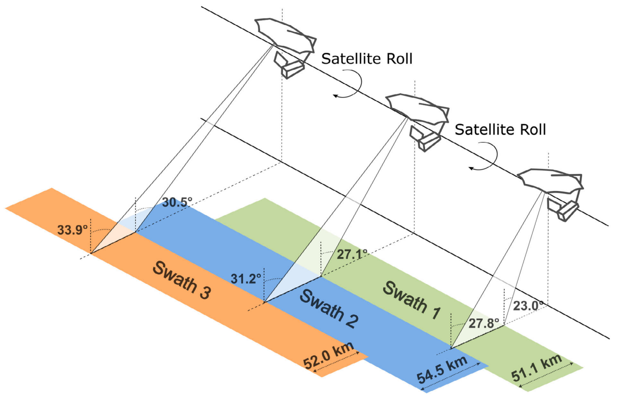

Fig. 4. ***BIOMASS operates in a strip map mode covering three swaths that will be accessed by roll maneuvers of the platform.***

Table 2 Biomass Transponder Specification

Parameter	Specification
Antenna Beam	12 deg HPBW. Gain 22.7 dBi
Simulated RCS	85 dB(m2) with an uncertainty $<$ 0.2 dB (1σ)
Gain stability	$<$ 0.1 dB (1σ) over the entire mission lifetime
Sensitivity	Capability to detect PFD $>$ -90 dBm/m2
Cross-Polar isolation	$<$ 40 dB (1-way) in both Tx and Rx
Channel Imbalance	$<$ 0.1 dB (1σ) in amplitude and $<$ 0.77 deg (1σ) in phase, including the antenna (2-way)
Signal to Multipath Ratio	$>$ 43.5 dB
Absolute pointing error	$<$ 0.5 deg (3σ) azimuth and elevation combined

(Fig. 5). The antenna can be steered in azimuth and elevation to track BIOMASS during the satellite overpasses. To ensure a high system performance and stability, the BCT contains an internal calibration network and an external calibration disk with a known radar cross section (RCS). BCT specifications are given in Table 2.

IV. MISSION OPERATION

A. BIOMASS Orbit

BIOMASS flies in a dawn-dusk sun-synchronous drifting orbit with a mean altitude of 666 km, an inclination of 97.97°, and a local time of the ascending node (LTAN) at 06:00 A.M., completing 14 + 2/3 revisions per day. The orbit's near-repeat cycle is three days, where the exact repeat position slightly deviates due to the drift. The actual drift and its direction depend on the mission phase and are specified in Sections IV-A and IV-B. The drift results in controlled interorbit distances (baselines) between successive revisits to the same site, which enables the Pol-InSAR and tomographic processing of the data. The ground track of the satellite is controlled to be within 10% of the critical baseline, which is approximately ±480 m.

B. In-Orbit Commissioning Phase

Following the launch and early orbit phase (LEOP), which took nine days and included the platform switch-on and the deployment of the LDR, the in-orbit commissioning phase (COM) started. This phase aimed at a complete characterization of the platform and payload performance to verify that the system was ready for the transition into the routine operations phase.

During this phase, the satellite, including the payload, was brought into a fully operational state. Relevant adjustments were made to the payload operational parameters and software to optimize its performance. The requirement of repeated passes over the BCT during this phase resulted in a dedicated orbit that differs slightly from the operational orbit, by around 30–300 m depending on the COM phase (Table 3). The COM phase lasted about six months and was split into six subphases, each characterized by a dedicated orbit.

COM-0 was the LEOP during which the platform was commissioned, and instrument functional checks were carried out. COM-1 was dedicated to a full instrument check to determine instrument health and readiness and to check out the operation of the BCT with BIOMASS. COM-2 was dedicated to the antenna pattern characterization using the BCT. This focused on acquiring 21 azimuth antenna pattern cuts of the individual doublets at different elevation angles as BIOMASS flew over the BCT. Biomass operated in a specific mode over the BCT to enable the two doublet patterns to be characterized. Following the collection of the 21 azimuth antenna cuts, the characterized doublet antenna secondary patterns were generated. This was used by the image processor together with the internal calibration data and ground characterization data to form the characterized antenna secondary patterns (CASPs). The comparison of the CASP with the combined pattern from the reference antenna secondary pattern (RASP) was

Fig. 5. ***BCT 2-D antenna array and housing, ©C-Core Canada.***

Table 3 Biomass System Commissioning Phases

Sub-Phase	Orbit type / requirements	Task duration
COM-0	From end of LEOP, on the move to Zero Drift orbit	30 days
COM-1	Zero Drift orbit, Swath-1	18 + 9 days for manoeuvres; 7 BCT revisits
COM-2	Swath-1, westward drifting orbit with a 3.42 km drift / 3 days	60 + 9 days for manoeuvres; 21 BCT revisits.
COM-3	Swath-1, eastward drifting orbit with a 6.875 km drift / 3 days	24 + 3 days for manoeuvres; 8 BCT revisits
COM-4	Pseudo TOM, Swath-2, eastward drifting orbit with a 0.887 km drift / 3 days	18 + 9 days for manoeuvres; 7 BCT revisits
COM-5	Pseudo TOM, Swath-3, eastward drifting orbit with a 0.887 km drift / 3 days	18 days; 7 BCT revisits

then performed to determine the pointing. COM-3 foresaw further calibration and verification activities. Following the antenna pattern and pointing characterization, this phase used the point target formed by the transponder operating in echo generation mode. The same echo data were used for polarimetric and radiometric calibration activities. COM-4 and COM-5 were finally dedicated to the calibration/verification of Swaths 2 and 3. During the different COM phases, each phase was dedicated to one of the three BIOMASS swaths and the satellite flew in dedicated orbits.

The BIOMASS commissioning phase was also a unique opportunity to investigate subsurface ice structure over Antarctica by means of P-band SAR tomography. Due to the relatively large drift during COM-2 and COM-3, the baselines achieved at high latitudes were more favorable for tomographic processing than those during the nominal mission phases. It must, however, be noted that due to the need to observe the BCT, full coverage of Antarctica could not be achieved during the COM phase (Fig. 6).

C. Nominal Mission Phases

To achieve the mission objectives, BIOMASS operates in two phases. Following the initial six-month commissioning phase, the mission proceeded with the tomographic phase (TOM) of 18 months on November 21, 2025. The TOM phase will be followed by the interferometric phase (INT) of 42 months, which will complete the mission's five-year operational lifetime. During the TOM phase, an interferometric stack (STA) of seven images is collected for each point within the TOM acquisition mask. In the INT phase, an interferometric STA of three images will be collected for each point within the INT acquisition mask. For both phases, the temporal repeat cycle between images of an STA is three days.

The drift during these phases and hence the horizontal baselines between successive revisits to the same site is 0.87 km (15% of the critical baseline) during the TOM phase, which translates to a height of ambiguity of 160 m and a vertical resolution of 25 m, and 1.49 km (30% of the critical baseline) during the INT phase, which translates to a height of ambiguity of 100 m. The baselines are defined at the equator and will reduce with latitude.

After completing an interferometric or tomographic STA, the platform performs a roll maneuver to access an adjacent swath. This pattern is repeated to cover the three swaths, forming a major cycle (MC) of the mission that takes 63 days during the TOM phase and 27 days during the INT phase. The overlap between the different swaths guarantees the generation of a seamless STA with some overlap between the STAs, which is subject to the orbit control uncertainty. Since the total equatorial swath imaged during an MC is insufficient for global coverage

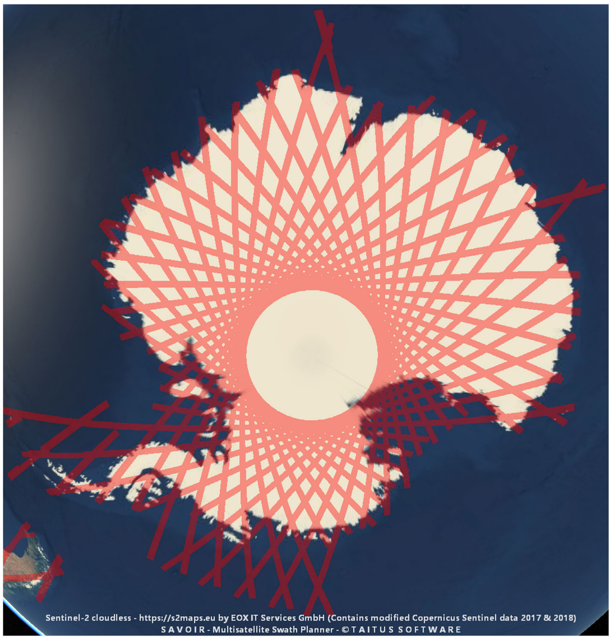

Fig. 6. *Antarctica acquisition footprints during COM-2 and COM-3.*

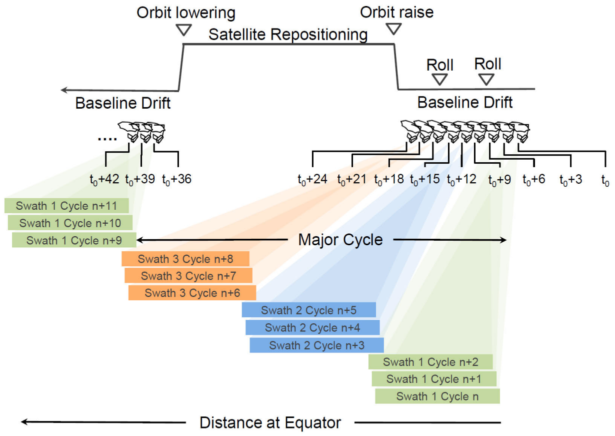

Fig. 7. ***Build-up of one MC during the INT mission phase. The build-up during the TOM mission phase is equivalent.***

at the equator, a satellite repositioning maneuver (SRM) is conducted to shift the satellite's ground track. This is achieved by raising the orbit by about 2 km relative to the nominal operational altitude to induce a fast westward drift. Once the required drift distance is achieved, the orbit is lowered back to the nominal altitude to start another MC in Swath 1 geometry, accessing the next ground region to be imaged (Fig. 7). For the TOM and INT phases, the orbit drift phase lasts 9 and 12 days, respectively. During the SRM's drifting phase, the SAR will acquire images over secondary target areas. After seven MCs, a global cycle (GC) is completed, covering the entire globe. The duration of a GC for the TOM phase is hence 504 days, and for the INT phase, it is 273 days.

D. Acquisition Planning

BIOMASS aims to cover forested areas between 75°N and 56°S. The BIOMASS mission is a secondary user of the allotted frequency band and is subject to ITU-imposed constraints on both the power flux density of transmissions at the Earth's surface and restrictions on the regions in which the SAR can be operated. Its coverage is restricted since BIOMASS is not currently allowed to operate within the line of sight of U.S. Department of Defense Space Object Tracking Radar (SOTR) radars. This mainly excludes the North American continent and Europe (Fig. 8). The impact of this restriction has been assessed and found not to compromise the mission objectives and scientific goals [47]. For the primary acquisition mask, data will be collected systematically, resulting in complete coverage for both ascending and descending passes. During its five years of operations, BIOMASS will hence systematically acquire one global coverage with TOM STAs and five global coverages with INT STAs in both ascending and descending geometries. It is important to note that the acquisition plan is quasi-frozen. The unusual acquisition build-up and the need to acquire STAs with a three-day temporal repeat cycle do not allow additional constraints to be ingested in the mission planning, such as observation of targets during specific time windows or seasons.

For secondary applications, data will be collected on a best effort basis after covering the primary objectives, with priorities defined in [44]. Secondary areas cover arid areas, Antarctica, and regions of interest in the ocean that are characterized by strong currents, salinity gradients, or sea ice for which P-band observations could be of interest (Fig. 8).

V. PRODUCTS AND PROCESSING

The BIOMASS Processing Suite (BPS) processes Level-0 data up to Level-2, generating a wide range of products. The documentation detailing the L1 and L2 processing algorithms, configuration parameters, and product format specification is available online at https://earth.esa.int/eogateway/missions/biomass/documentation, while the software can be downloaded at https://github.com/BioPAL/BPS. The product tree with the different product levels and types is illustrated in Fig. 9. The processing involves the following steps.

1) *L1a/b Processing:* This is the BIOMASS image formation step, going from raw data to focused images. This includes, e.g., compensation of antenna pattern, suppression of RFI artifacts, and the first compensation of ionosphere effects. The ionospheric calibration step is key to ensuring the quality of BIOMASS data and was specially designed for the mission. Two kinds of corrections are foreseen in the L1 Processor framework: correction of Faraday rotation (FR) and correction of ionosphere-induced phase distortions [48].
2) *L1c Processing:* This is the interferometric processing that generates the seven-image tomographic STAs or the three-image interferometric STAs. It includes the coregistration of the images, filtering of the common Doppler spectrum, and phase calibration steps to compensate for residual ionosphere and baseline errors. It also includes computation of the ground steering phase required for subsequent processing steps (e.g., L2 or digital terrain model (DTM) generation), which is done by means of sum of Kronecker

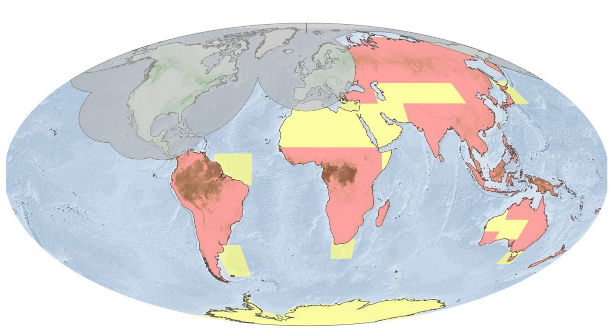

Fig. 8. ***Observation mask covers primary objective areas in red, secondary objective areas in yellow, and the SOTR exclusion zones in gray shaded areas.***

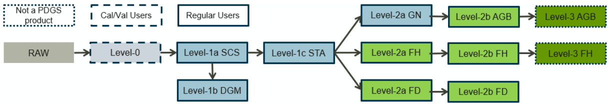

Fig. 9. ***Product tree for the BIOMASS mission.***

products (SKP) decomposition [49]. The SKP calibration step aims to compensate the ground phase and residual disturbances. The L1c processing uses the Copernicus DEM as input, e.g., for geometric coregistration and computation of flattening phase screen. Once the BIOMASS-derived DTM is available, it will also be considered for supporting the L1c processing.

3) *L2a Processing:* Intermediate L2 processing performed for each STA. For one GC, the number of STAs varies mainly with latitude, approximately from a minimum of two at the Equator (ascending/descending) to about six at higher latitudes (three ascending/descending pairs) [50].

4) *L2b Processing:* This processing aggregates, for each GC, all the L2a products covering the same location on the ground, generating a single BIOMASS L2b product tile. A different number of STAs may be available for each geographic grid tile, depending on swath coverage with respect to grid tiling.

5) *L3 Processing:* This processing improves the consistency of L2b maps by enforcing geophysical constraints through an iterative statistical regularization process. The processor is currently being developed and will be integrated in the BPS once validated with real BIOMASS data at the end of the second global coverage around the end of 2027. Fig. 10 shows the different product characteristics. L1a/b/c and L2a coverage corresponds to standard image frames, whereas L2b will be delivered on a $1^\circ \times 1^\circ$ global grid tiling combining all available frames from ascending and descending acquisitions in a single product. The core scientific processing suite for the L1c calibrator and L2a/b products is maintained as an open-source library, allowing the scientific community to access the code and directly contribute to the evolution of the processors (https://www.biomass-disk.info/biopal, https://github.com/BioPAL)

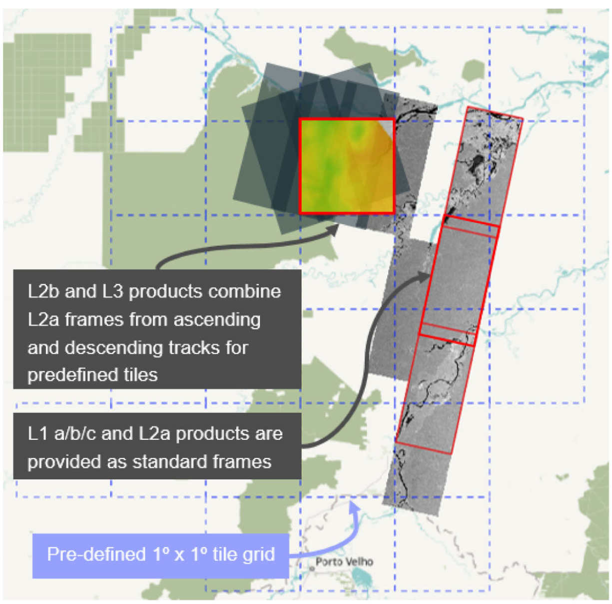

Fig. 10. ***Schematic of the L1 a/b/c and L2a products in standard frame geometry and L2b tile products.***

Within these product levels, the BIOMASS BPS product family includes the following.

1) *L1a or Single-Look Complex Slant Range (SCS):* L1a products are images in the slant range versus azimuth plane, i.e., in the image plane of satellite data acquisition. Each pixel is represented by a complex value containing calibrated radar amplitude and phase. The processing for all L1a products results in a single look in each dimension using the full available signal bandwidth. L1a images are produced in a Zero-Doppler geometry. This convention is common with the standard slant-range products available from other SAR sensors. The L1a products contain one image per polarization channel. The L1a image is sampled at the natural pixel spacing in range (i.e., the radar range sampling frequency) and at a configurable pixel spacing in azimuth. Examples of polarimetric HSI images are given in Fig. 11.

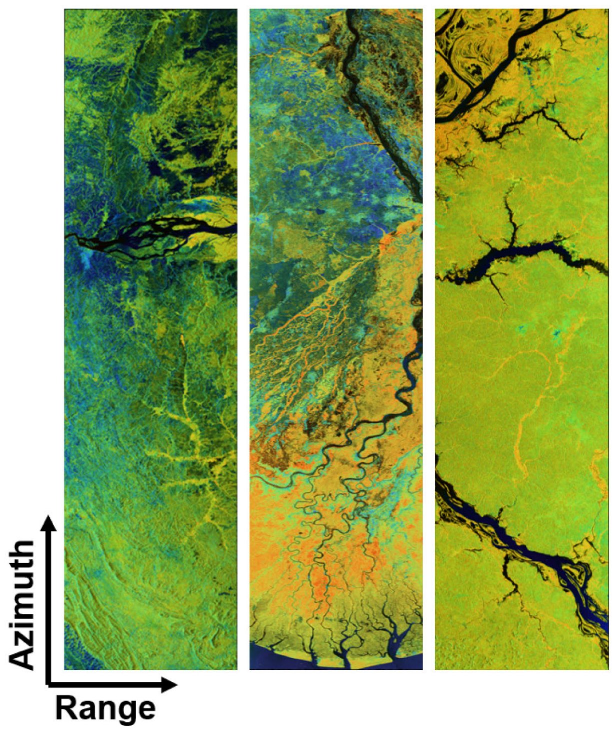

Fig. 11. ***BIOMASS polarimetric HSI image from Kongo River, Niger Delta, and the Amazon (from left to right).***

2) *L1b or Detected Ground-Range Multilooked (DGM):* L1b products lie in the ground range versus azimuth plane, with image coordinates oriented along ground range and flight direction. The standard L1b products are detected, multilook products (six looks), with square resolution cells and square pixel spacing. The resolution of the product will be 50 × 50 m^2. Each image pixel is represented by a real (amplitude) value, which can be translated to calibrated radar brightness. Thermal noise compensation is not applied by default on data, but the information to perform the procedure is included in the metadata.
3) *L1c or Coregistered STA:* L1c products are obtained by coregistering a given L1a image to a reference L1a image. The coregistration operation consists in a bidimensional interpolation of the data over a reference sampling grid. From a product definition perspective, L1c products are very similar to L1a ones. The only exception is the number of polarizations, which can be either 4 or 3, since cross-polarization channels can be combined, e.g., to improve SNR. A specificity of this product is that L1c images are stored independently and not as STA files.
4) *L2a (STA-Based Biophysical Product):* L2a products are biophysical properties. There is no dependency between different L2a products, and they can be considered as a biophysical extension of the STA products (L1c). The products are geocoded and are obtained from a single STA. There are three L2a products.
   a) *FD:* The FD L2a product represents forest change between two GCs. Deforested or logged areas are defined as an area where a patch of forest has been cleared to zero biomass (or below the sensitivity limit for BIOMASS). The product has a resolution of 50 × 50 m^2. The FD product has a finer resolution because less sensitivity is needed to detect the large backscatter changes associated with deforestation.
   b) *FH:* The FH L2a products represent the top canopy height (TCH). It is envisaged that the INT and TOM phases will use the same algorithms to generate this product, which in both phases will be based on a three-image STA. The product has a resolution of 200 × 200 m^2.
   c) *Ground Notch (GN):* The GN L2a is a preprocessing product of the L2b AGBD product. This product represents ground-canceled data, i.e., a signal processing filter is applied on the three-image STA, which cancels the signal contribution from the ground layer and enhances the signal contribution from the above-ground volume layer [51]. It is envisaged that the INT and TOM phases will both use the same algorithms to generate this product from a three-image STA. The product has a resolution of 200 × 200 m^2.
5) *L2b (Tile-Based Biophysical Product):* L2b products are biophysical, geocoded, and tile-based. They are derived from merging all L2a products from a given GC on the tile. The products at this level can take advantage of FD availability (for the same geographic tile) or of a forest mask generated outside the BPS to mask out nonforest pixels. The products are given as follows.
   a) *FD:* The FD L2b product is similar to the L2a FD product but combines acquisitions from ascending and descending acquisitions and overlapping areas. It also contains the aggregation of the probability change map and a computed forest mask. The product has a resolution of 50 × 50 m^2.
   b) *FH:* The FH L2b product is similar to the L2a FH product but combines ascending and descending acquisitions and overlapping areas using weighted averaging and feathering. An aggregated quality indicator is also provided. The product has a resolution of 200 × 200 m^2.
   c) *Above-Ground Biomass Density*: The AGBDL2b product represents above-ground dry biomass per unit area in tons/ha and its quality layer in a geographic tile (latitude–longitude) retrieved from L2a GN. The product combines acquisitions and overlapping areas [52]. The product has a resolution of 200 × 200 m^2.

Level-1 and Level-2 products will be routinely processed during the TOM and INT phases in the ESA ground segment. Products will be free and open in a cloud-friendly data format based on Cloud Optimized GeoTIFF (COG) and SpatioTemporal Asset Catalog (STAC) metadata.

A Level-3 processor is also under development and will be able to provide consolidated global biophysical parameters (AGBD and FH). The L3 products are planned to be delivered after completing a GC and will respect the same tiling concept in place for L2b products. The L3 processor aims at ensuring temporal consistency by constraining L3 variations over different GCs and spatial consistency by regularizing spatial anomalies. It also targets consistency between FH and AGBD estimates using local regression. The production model for Level-3 products is currently being consolidated.

Biophysical Level-2 and Level-3 products will be fully validated using data from the GeoTrees project. This project plans to establish 100 Reference Measurement Sites across the tropics, encompassing forest census, airborne, and terrestrial lidar measurements (https://geotrees.org/)

BIOMASS follows ESA's open data policy for its Earth Explorer missions. Level-1, Level-2, and Level-3 data will be fully free and open through ESA's Earth Observation Gateway (https://earth.esa.int/eogateway). Level-0 data will follow the same approach but will only be shared following a data release request through the ESA Tellus system (https://esatellus.service-now.com/). In addition to this traditional way of accessing BIOMASS data, data can also be accessed through the BIOMASS MAAP platform, which is a novel infrastructure providing access to data and computing resources for ESA's new Explorer missions (https://portal.maap.eo.esa.int/biomass/)

VI. SECONDARY APPLICATIONS

BIOMASS carries the first spaceborne P-band SAR, which provides unprecedented observational capabilities that naturally enable a variety of secondary applications beyond its primary objectives. These opportunities arise as beneficial by-products of the mission's unique instrumentation rather than as drivers of its design. BIOMASS will provide valuable observational data for ice sheets, deserts, the ionosphere, below canopy topography, and other domains. BIOMASS will complement operational ice sheet velocity mapping [53], [54], because its left-looking geometry ensures a smaller polar gap in Antarctica than most existing SAR satellites. Also, its lower frequency ensures longer coherence time due to deeper penetration [55], which favors interferometry and results in less noisy velocity maps. This is crucial in the interior of Antarctica, where the current ice velocity error can be three times larger than the velocity itself [56]. Finally, the low frequency facilitates phase unwrapping, especially for fast-flowing glaciers, which tend to decorrelate because of large velocity gradients in shear zones [57]. Structural mapping of ice sheets and ice shelves also benefits from the deeper penetration at P band and the Pol-InSAR and TomoSAR phases of the BIOMASS mission. With airborne P-band TomoSAR and Pol-InSAR, ice sheet structure and basal topography of up to 120-m-thick ice have successfully been mapped [58], [59], [60], [61]. This will provide new insight on firn depth and density and its meltwater absorption capacity [62] and on the contribution of runoff to mass balance, as well as the stability of ice sheets and ice shelves. The basal topography is of interest to understand the impact of basal canals on the stability of ice shelves and gain detailed information on the grounding zone.

Over arid regions, low-frequency spaceborne SAR has the capability to image subsurface features down to several meters. A first demonstration of this capability was performed in Egyptian desert during the early eighties [63] and, more recently, L-band SAR satellites, such as the Japanese ALOS and ALOS-2, allowed the mapping of vast ancient hydrographic systems in Northern Africa [64], [65], southern Mongolia [66], and Namibia [67]. Compared to existing L-band sensors, the BIOMASS P-band SAR should be able to probe even deeper into the subsurface, down to more than 5 m, as was demonstrated from airborne P-band SAR acquisitions over a desert site in southern Tunisia [68], opening a new era in terrestrial desert study.

As an integral part of its ability to make height-resolved measurements in forest canopies, the tomographic phase of the mission will gain access to a true DTM that is unaffected by forest cover [69]. Since global tomographic acquisitions occupy the first phase of the mission, this improved DTM will be available early in the interferometric phase and, besides its general use, will improve the BIOMASS L2 biophysical products.

Finally, BIOMASS will yield new insights on the ionosphere. The high susceptibility of P band to the electron content of the ionosphere will provide new observations along the orbit based on SAR polarimetry [70], [71] and interferometric techniques [72] at spatial resolutions of around a kilometer, giving an unprecedented capability to measure spatial structures and their changes, since they will be viewed every 2 h as the orbit repeats. The dawn-dusk orbit will cover major features, including the quiescent ionosphere at low latitudes and mid-latitudes, steep gradients around the dusk-side mid-latitude trough, and large irregularities in the auroral ovals and the polar cap.

VII. CONCLUSION

The ESA's BIOMASS mission is an innovative Earth observation satellite mission launched on April 29, 2025. Use of a P-band SAR will allow the BIOMASS radar to penetrate dense forest canopies and to capture structural data even in these challenging environments. The mission will operate in two phases: the tomographic phase and the interferometric phase, supporting advanced SAR imaging techniques.

BIOMASS will deliver estimates of FH and above-ground biomass at 200×200 m^2 resolutions and loss dynamics at 50×50 m^2 resolution for the largely underobserved and vulnerable forest areas worldwide. Its novel monitoring capabilities pave the way to greatly improve quantitative understanding of forest dynamics and constrain estimates of terrestrial carbon fluxes in the land surface models that underpin Earth system models [73], [74]. Further, by improving the representation of mortality, disturbance, and regrowth dynamics, BIOMASS will help to reduce the current large uncertainties in forest models [75] and the representation of the future trajectory of the land carbon cycle [76]

The science driver of BIOMASS is the role of forest in the Earth's carbon cycle, but this has naturally led to the mission using pioneering space technology, advanced instrumentation, and innovative methods. It is the first civilian P-band in space and the first mission to support the systematic exploitation of Pol-InSAR and TomoSAR processing. These unique capabilities open the door to opportunistic and unanticipated applications extending beyond the mission's core science goals and make the mission a true Earth Explorer. ■

REFERENCES

[1] *Earth Science in Action for Tomorrow's World Earth Observation Science Strategy*, European Space Agency, Frascati, Italy, Oct. 2024. [Online]. Available: https://esamultimedia.esa.int/docs/EarthObservation/ESA_Earth_Observation_Science_Strategy_issued_Sept_2024.pdf

[2] G. B. Bonan, "Forests and climate change: Forcings, feedbacks, and the climate benefits of forests," *Science*, vol. 320, no. 5882, pp. 1444–1449, Jun. 2008, doi: 10.1126/science.1155121.

[3] Y. Pan et al., "A large and persistent carbon sink in the World's forests," *Science*, vol. 333, no. 6045, pp. 988–993, Aug. 2011, doi: 10.1126/science.1201609.

[4] Y. Malhi et al., "The carbon balance of tropical forest regions, 1990–2005," *Glob. Chang. Biol.*, vol. 26, no. 1, pp. 1–14, 1990, doi: 10.1111/gcb.14817.

[5] W. Hubau et al., "Asynchronous carbon sink saturation in African and Amazonian tropical forests," *Nature*, vol. 579, no. 7797, pp. 80–87, Mar. 2020, doi: 10.1038/s41586-020-2035-0.

[6] R. J. W. Brienen et al., "Long-term decline of the Amazon carbon sink," *Nature*, vol. 519, no. 7543, pp. 344–348, Mar. 2015, doi: 10.1038/nature14283.

[7] R. A. Houghton, "Carbon emissions and the drivers of deforestation and forest degradation in the tropics," *Current Opinion Environ. Sustainability*, vol. 4, no. 6, pp. 597–603, Dec. 2012, doi: 10.1016/j.cosust.2012.06.006.

[8] M. Reichstein et al., "Climate extremes and the carbon cycle," *Nature*, vol. 500, no. 7462, pp. 287–295, Aug. 2013, doi: 10.1038/nature12350.

[9] C. D. Allen et al., "A global overview of drought and heat-induced tree mortality reveals emerging climate change risks for forests," *Forest Ecol. Manage.*, vol. 259, no. 4, pp. 660–684, Feb. 2010, doi: 10.1016/j.foreco.2009.09.001.

[10] L. Fan et al., "Negative asymmetric response of pantropical gross primary productivity to precipitation anomalies," *Earth's Future*, vol. 12, no. 10, Oct. 2024, doi: 10.1029/2024ef004760.

[11] S. Botía et al., "Reduced vegetation uptake during the extreme 2023 drought turns the Amazon into a weak carbon source," *AGU Adv.*, vol. 7, no. 1, Feb. 2026, doi: 10.1029/2025av001658.

[12] P. Friedlingstein, "Global carbon budget 2024," *Earth Syst. Sci. Data*, vol. 17, no. 3, pp. 965–1039, 2025, doi: 10.5194/essd-17-965-2025.

[13] H. Fang et al., "Satellite-based monitoring of China's above-ground biomass carbon sink from 2015 to 2021," *Agricult. Forest Meteorol.*, vol. 356, Sep. 2024, Art. no. 110172, doi: 10.1016/j.agrformet.2024.110172.

[14] H. Yang et al., "Global increase in biomass carbon stock dominated by growth of northern young forests over past decade," *Nature Geosci.*, vol. 16, no. 10, pp. 886–892, Oct. 2023, doi: 10.1038/s41561-023-01274-4.

[15] L. Yu et al., "Forest degradation contributes more to carbon loss than forest cover loss in North American boreal forests," *Int. J. Appl. Earth Observ. Geoinf.*, vol. 128, Apr. 2024, Art. no. 103729, doi: 10.1016/j.jag.2024.103729.

[16] L. Fan et al., "Siberian carbon sink reduced by forest disturbances," *Nature Geosci.*, vol. 16, no. 1, pp. 56–62, Jan. 2023, doi: 10.1038/s41561-022-01087-x.

[17] W. R. L. Anderegg et al., "Tree mortality from drought, insects, and their interactions in a changing climate," *New Phytologist*, vol. 208, no. 3, pp. 674–683, Nov. 2015, doi: 10.1111/nph.13477.

[18] M. Reichstein and N. Carvalhais, "Aspects of forest biomass in the Earth system: Its role and major unknowns," *Surveys Geophysics*, vol. 40, no. 4, pp. 693–707, Jul. 2019, doi: 10.1007/s10712-019-09551-x.

[19] F. J. Fischer et al., "A simulation method to infer tree allometry and forest structure from airborne laser scanning and forest inventories," *Remote Sens. Environ.*, vol. 251, Dec. 2020, Art. no. 112056, doi: 10.1016/j.rse.2020.112056.

[20] L. Terryn et al., "Quantifying tropical forest structure through terrestrial and UAV laser scanning fusion in Australian rainforests," *Remote Sens. Environ.*, vol. 271, Mar. 2022, Art. no. 112912, doi: 10.1016/j.rse.2022.112912.

[21] L. Terryn et al., "New tree height allometries derived from terrestrial laser scanning reveal substantial discrepancies with forest inventory methods in tropical rainforests," *Global Change Biol.*, vol. 30, no. 8, Aug. 2024, doi: 10.1111/gcb.17473.

[22] W. Yang, P. Wilkes, M. B. Vicari, K. Hand, K. Calders, and M. Disney, "Treegraph: Tree architecture from terrestrial laser scanning point clouds," *Remote Sens. Ecol. Conservation*, vol. 10, no. 6, pp. 755–774, Dec. 2024, doi: 10.1002/rse2.399.

[23] M. Santoro et al., "Design and performance of the climate change initiative biomass global retrieval algorithm," *Sci. Remote Sens.*, vol. 10, no. 100169, 2024, doi: 10.1016/j.srs.2024.100169.

[24] L. Duncanson et al., "Aboveground biomass density models for NASA's global ecosystem dynamics investigation (GEDI) LiDAR mission," *Remote Sens. Environ.*, vol. 270, Mar. 2022, Art. no. 112845, doi: 10.1016/j.rse.2021.112845.

[25] J.-P. Wigneron et al., "SMOS-IC data record of soil moisture and L-VOD: Historical development, applications and perspectives," *Remote Sens. Environ.*, vol. 254, Mar. 2021, Art. no. 112238, doi: 10.1016/j.rse.2020.112238.

[26] M. Santoro et al., "The global forest above-ground biomass pool for 2010 estimated from high-resolution satellite observations," *Earth Syst. Sci. Data*, vol. 13, no. 8, pp. 3927–3950, 2021, doi: 10.5194/essd-13-3927-2021. [Online]. Available: https://www.earth-system-science-data.net/

[27] W. Qi et al., "Mapping large-scale pantropical forest canopy height by integrating GEDI lidar and TanDEM-X InSAR data," *Remote Sens. Environ.*, vol. 318, 2025, Art. no. 114488, doi: 10.1016/j.rse.2024.114488. [Online]. Available: https://www.sciencedirect.com/science/article/pii/S0034425724005601

[28] R. Guliaev, J. Su Kim, M. Pardini, and K. P. Papathanassiou, "On the use of tomographically derived reflectivity profiles for pol-InSAR forest height inversion in the context of the BIOMASS mission," *IEEE Trans. Geosci. Remote Sens.*, vol. 62, 2024, Art. no. 5228712, doi: 10.1109/TGRS.2024.3497572.

[29] F. Kugler, S.-K. Lee, and K. P. Papathanassiou, "Estimation of forest vertical sructure parameter by means of multi-baseline pol-InSAR," in *Proc. IEEE Int. Geosci. Remote Sens. Symp.*, Apr. 2009, pp. V-721–V-724, doi: 10.1109/IGARSS.2009.5417478.

[30] S. R. Cloude and K. P. Papathanassiou, "Polarimetric SAR interferometry," *IEEE Trans. Geosci. Remote Sens.*, vol. 36, no. 5, pp. 1551–1565, Sep. 1998, doi: 10.1109/36.718859.

[31] S. Tebaldini, "Single and multipolarimetric SAR tomography of forested areas: A parametric approach," *IEEE Trans. Geosci. Remote Sens.*, vol. 48, no. 5, pp. 2375–2387, May 2010, doi: 10.1109/TGRS.2009.2037748.

[32] S. Tebaldini, D. Ho Tong Minh, M. M. d'Alessandro, L. Villard, T. Le Toan, and J. Chave, "The status of technologies to measure forest biomass and structural properties: State of the art in SAR tomography of tropical forests," *Surv. Geophys.*, vol. 40, no. 4, pp. 779–801, Jul. 2019, doi: 10.1007/s10712-019-09539-7.

[33] M. Pardini, M. Tello, V. Cazcarra-Bes, K. P. Papathanassiou, and I. Hajnsek, "L- and P-band 3-D SAR reflectivity profiles versus LiDAR waveforms: The AfriSAR case," *IEEE J. Sel. Topics Appl. Earth Observ. Remote Sens.*, vol. 11, no. 10, pp. 3386–3401, Oct. 2018, doi: 10.1109/JSTARS.2018.2847033.

[34] T. Le Toan et al., "The BIOMASS mission: Mapping global forest biomass to better understand the terrestrial carbon cycle," *Remote Sens. Environ.*, vol. 115, no. 11, pp. 2850–2860, Nov. 2011, doi: 10.1016/j.rse.2011.03.020.

[35] S. Quegan et al., "The European space agency BIOMASS mission: Measuring forest above-ground biomass from space," *Remote Sens. Environ.*, vol. 227, pp. 44–60, Jun. 2019, doi: 10.1016/j.rse.2019.03.032.

[36] D. Schimel et al., "Observing terrestrial ecosystems and the carbon cycle from space," *Global Change Biol.*, vol. 21, no. 5, pp. 1762–1776, May 2015, doi: 10.1111/gcb.12822.

[37] L. Duncanson et al., "Spatial resolution for forest carbon maps," *Science*, vol. 387, no. 6732, pp. 370–371, Jan. 2025, doi: 10.1126/science.adt6811.

[38] J. Reiche et al., "Combining satellite data for better tropical forest monitoring," *Nat. Clim. Chang.*, vol. 6, pp. 120–122, 2016, doi: 10.1038/nclimate2919.

[39] M. C. Hansen et al., "High-resolution global maps of 21st-century forest cover change," *Science*, vol. 342, no. 6160, pp. 850–853, Nov. 2013, doi: 10.1126/science.1244693.

[40] E. T. A. Mitchard et al., "Uncertainty in the spatial distribution of tropical forest biomass: A comparison of pan-tropical maps," *Carbon Balance Manag.*, vol. 14, no. 1, pp. 1–13, 2019, doi: 10.1186/s13021-019-0129-5.

[41] L. Duncanson et al., "The importance of consistent global forest aboveground biomass product validation," *Surv. Geophys.*, vol. 40, no. 4, pp. 979–999, Jul. 2019, doi: 10.1007/s10712-019-09538-8.

[42] C. Warren, C. Lloyd, and M. Fehringer, "Overview of the biomass satellite," in *Proc. IEEE Int. Geosci. Remote Sens. Symp.*, Jul. 2018, pp. 8567–8570, doi: 10.1109/IGARSS.2018.8518306.

[43] T. Fugen et al., "The biomass SAR instrument: Development status and performance overview," in *Proc. IEEE Int. Geosci. Remote Sens. Symp. (IGARSS)*, Valencia, Spain, 2018, pp. 8571–8574, doi: 10.1109/IGARSS.2018.8518041.

[44] *Biomass Mission Requirement Document V5.0*, ESA, Noordwijk, The Netherlands, Aug. 2016.

[45] J. S. Kim and K. Papathanassiou, "Cross-talk calibration of polarimetric SAR under Faraday rotation," in *Proc. IEEE Int. Geosci. Remote Sens. Symp. (IGARSS)*, Jul. 2024, pp. 2411–2413, doi: 10.1109/IGARSS53475.2024.10641164.

[46] S. Quegan et al., "Calibration challenges for the biomass P-band SAR instrument," in *Proc. IGARSS - IEEE Int. Geosci. Remote Sens. Symp.*, Jul. 2018, pp. 8575–8578, doi: 10.1109/IGARSS.2018.8518646.

[47] J. M. B. Carreiras et al., "Coverage of high biomass forests by the ESA BIOMASS mission under defense restrictions," *Remote Sens. Environ.*, vol. 196, pp. 154–162, May 2017, doi: 10.1016/j.rse.2017.05.024.

[48] P. Prats-Iraola et al., "The BIOMASS ground processor prototype: An overview," in *Proc. Eur. Conf. Synth. Aperture Radar, EUSAR, Aachen*, 2018, pp. 1–6.

[49] F. Banda et al., "Biomass interferometric calibration processor design," in *Proc. IEEE Int. Geosci. Remote Sens. Symp. (IGARSS)*, Jul. 2023, pp. 7785–7788, doi: 10.1109/IGARSS52108.2023.10283343.

[50] F. Banda et al., "The BIOMASS level 2 prototype processor: Design and experimental results of above-ground biomass estimation," *Remote Sens.*, vol. 12, no. 6, p. 985, Mar. 2020, doi: 10.3390/rs12060985.

[51] M. M. d'Alessandro, S. Tebaldini, S. Quegan, M. J. Soja, L. M. H. Ulander, and K. Scipal, "Interferometric ground cancellation for above ground biomass estimation," *IEEE Trans. Geosci. Remote Sens.*, vol. 58, no. 9, pp. 6410–6419,

Sep. 2020, doi: 10.1109/TGRS.2020.2976854.
[52] M. J. Soja et al., "Mapping above-ground biomass in tropical forests with ground-cancelled P-band SAR and limited reference data," *Remote Sens. Environ.*, vol. 253, Feb. 2021, Art. no. 112153, doi: 10.1016/j.rse.2020.112153.
[53] A. Solgaard et al., "Greenland ice velocity maps from the PROMICE project," *Earth Syst. Sci. Data*, vol. 13, no. 7, pp. 3491–3512, Jul. 2021, doi: 10.5194/essd-13-3491-2021.
[54] I. Joughin, B. E. Smith, and I. M. Howat, "A complete map of Greenland ice velocity derived from satellite data collected over 20 years," *J. Glaciol.*, vol. 64, no. 243, pp. 1–11, Feb. 2018, doi: 10.1017/jog.2017.73.
[55] E. Rignot, "Changes in west Antarctic ice stream dynamics observed with ALOS PALSAR data," *Geophys. Res. Lett.*, vol. 35, no. 12, Jun. 2008, doi: 10.1029/2008gl033365.
[56] E. Rignot, J. Mouginot, and B. Scheuchl, "Ice flow of the Antarctic ice sheet," *Science*, vol. 333, no. 6048, pp. 1427–1430, Sep. 2011, doi: 10.1126/science.1208336.
[57] I. Joughin, "Ice-sheet velocity mapping: A combined interferometric and speckle-tracking approach," *Ann. Glaciol.*, vol. 34, pp. 195–201, Sep. 2002, doi: 10.3189/172756402781817978.
[58] F. Banda, J. Dall, and S. Tebaldini, "Single and multipolarimetric P-band SAR tomography of subsurface ice structure," *IEEE Trans. Geosci. Remote Sens.*, vol. 54, no. 5, pp. 2832–2845, May 2016, doi: 10.1109/TGRS.2015.2506399.
[59] G. Fischer, K. P. Papathanassiou, and I. Hajnsek, "Modeling multifrequency pol-InSAR data from the percolation zone of the Greenland ice sheet," *IEEE Trans. Geosci. Remote Sens.*, vol. 57, no. 4, pp. 1963–1976, Apr. 2019, doi: 10.1109/TGRS.2018.2870301.
[60] G. Fischer, M. Jäger, K. P. Papathanassiou, and I. Hajnsek, "Modeling the vertical backscattering distribution in the percolation zone of the Greenland ice sheet with SAR tomography," *IEEE J. Sel. Topics Appl. Earth Observ. Remote Sens.*, vol. 12, no. 11, pp. 4389–4405, Nov. 2019, doi: 10.1109/JSTARS.2019.2951026.
[61] K. Wang et al., "A novel airborne TomoSAR 3-D focusing method for accurate ice thickness and glacier volume estimation," *ISPRS J. Photogramm. Remote Sens.*, vol. 220, pp. 593–607, Feb. 2025, doi: 10.1016/j.isprsjprs.2025.01.011.
[62] S. B. M. Veldhuijsen, W. J. van de Berg, M. Brils, P. K. Munneke, and M. R. van den Broeke, "Characteristics of the 1979–2020 Antarctic firn layer simulated with IMAU-FDM v1.2A," *Cryosphere*, vol. 17, no. 4, pp. 1675–1696, Apr. 2023, doi: 10.5194/tc-17-1675-2023.
[63] J. F. McCauley et al., "Subsurface valleys and geoarcheology of the eastern Sahara revealed by shuttle radar," *Science*, vol. 218, no. 4576, pp. 1004–1020, Dec. 1982, doi: 10.1126/science.218.4576.1004.
[64] P. Paillou, S. Lopez, T. Farr, and A. Rosenqvist, "Mapping subsurface geology in Sahara using L-band SAR: First results from the ALOS/PALSAR imaging radar," *IEEE J. Sel. Topics Appl. Earth Observ. Remote Sens.*, vol. 3, no. 4, pp. 632–636, Dec. 2010, doi: 10.1109/JSTARS.2010.2056915.
[65] C. Skonieczny et al., "African humid periods triggered the reactivation of a large river system in western Sahara," *Nature Commun.*, vol. 6, no. 1, p. 8751, Nov. 2015, doi: 10.1038/ncomms9751.
[66] T. Sternberg and P. Paillou, "Mapping potential shallow groundwater in the Gobi desert using remote sensing: Lake ulaan nuur," *J. Arid Environ.*, vol. 118, pp. 21–27, Jul. 2015, doi: 10.1016/j.jaridenv.2015.02.020.
[67] P. Paillou, S. Lopez, E. Marais, and K. Scipal, "Mapping Paleohydrology of the ephemeral Kuiseb river, namibia, from radar remote sensing," *Water*, vol. 12, no. 5, p. 1441, May 2020, doi: 10.3390/w12051441.
[68] P. Paillou et al., "Mapping of subsurface features in arid environments using P-band SAR: The TuniSAR campaign," in *Proc. Prog. Electromagn. Res. Symp. (PIERS)*, Marrakesh, Morocco, Mar. 2011, pp. 1171–1174.
[69] M. M. D'Alessandro and S. Tebaldini, "Retrieval of terrain topography in tropical forests using P-band SAR tomography," in *Proc. IEEE Int. Geosci. Remote Sens. Symp. (IGARSS)*, Jul. 2018, pp. 8598–8600, doi: 10.1109/IGARSS.2018.8518092.
[70] P. A. Wright, S. Quegan, N. S. Wheadon, and C. D. Hall, "Faraday rotation effects on l-band spaceborne SAR data," *IEEE Trans. Geosci. Remote Sens.*, vol. 41, no. 12, pp. 2735–2744, Dec. 2003, doi: 10.1109/TGRS.2003.815399.
[71] J. S. Kim and K. P. Papathanassiou, "TEC and ionospheric height estimation by means of azimuth subaperture analysis in quad-polarimetric spaceborne SAR data," *IEEE J. Sel. Topics Appl. Earth Observ. Remote Sens.*, vol. 14, pp. 6279–6290, 2021, doi: 10.1109/JSTARS.2021.3085130.
[72] S. Tebaldini, M. M. d'Alessandro, J. S. Kim, and K. Papathanassiou, "Ionosphere vertical profiling from biomass multi-squint InSAR," in *Proc. IEEE Int. Geosci. Remote Sens. Symp. (IGARSS)*, Jul. 2017, pp. 5866–5869, doi: 10.1109/IGARSS.2017.8128343.
[73] N. MacBean et al., "Quantifying and reducing uncertainty in global carbon cycle predictions: Lessons and perspectives from 15 years of data assimilation studies with the ORCHIDEE terrestrial biosphere model," *Global Biogeochemical Cycles*, vol. 36, no. 7, Jul. 2022, doi: 10.1029/2021gb007177.
[74] N. Raoult et al., "Parameter estimation in land surface models: Challenges and opportunities with data assimilation and machine learning," *J. Adv. Model. Earth Syst.*, vol. 17, no. 11, Oct. 2024, Art. no. e2024MS004733, doi: 10.22541/essoar.172838640.01153603/v1.
[75] H. Bugmann et al., "Tree mortality submodels drive simulated long-term forest dynamics: Assessing 15 models from the stand to global scale," *Ecosphere*, vol. 10, no. 2, Feb. 2019, doi: 10.1002/ecs2.2616.
[76] A. D. Friend et al., "Carbon residence time dominates uncertainty in terrestrial vegetation responses to future climate and atmospheric CO_2," *Proc. Nat. Acad. Sci. USA*, vol. 111, no. 9, pp. 3280–3285, Mar. 2014, doi: 10.1073/pnas.1222477110.

ABOUT THE AUTHORS

Klaus Scipal (Member, IEEE) received the Dipl.-Ing. degree in geodesy and the Ph.D. degree in technical sciences from Vienna University of Technology, Vienna, Austria, in 1999 and 2002, respectively.

He has been working as an Assistant Professor at the Institute of Photogrammetry and Remote Sensing, Vienna University of Technology, and a Research Consultant at European Centre for Medium-Range Weather Forecasts, Reading, U.K., in the fields of Earth observation and data assimilation with a focus on land surface processes. In 2009, he joined the Space Research and Technology Centre, European Space Agency (ESA), Noordwijk, The Netherlands, as a Mission Scientist working on the development of future SAR satellite concepts. In 2020, he was appointed as a Mission Manager for the SMOS and BIOMASS satellite missions at the Space Research Centre, ESA, Frascati, Italy.

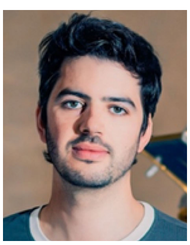

Clément Albinet received the Eng. degree from the École Centrale de Nantes, Nantes, France, the master's degree from the University of Nantes, Nantes, in 2008, and the Ph.D. degree from the University of Rennes, Rennes, France, in 2013.

He was involved in the definition of the BIOMASS mission from 2008 to 2015, during which he worked at CNES/CESBIO, Toulouse, France, and ONERA, Toulouse, on processing of P-band airborne campaign data, SAR instrumentation, and data modeling. In 2015, he joined European Space Agency (ESA), Frascati, Italy, to work on the sensor performance, products, and algorithms evolutions of SAR missions. He is currently based at European Space Research Institute (ESA-ESRIN), Rome, Italy, and is the Data Quality Manager of the BIOMASS mission.

Michele Caccia received the M.Sc. degree in telecommunication engineering from the Universitá Federico Secondo di Napoli, Naples, Italy, in 2010.

Since 2011, he has been working on synthetic aperture radar (SAR) processing, calibration, quality control, and applications, including Sentinel-1 and BIOMASS. He started working on BIOMASS in 2019 as a PDGS Instrument Engineer, supporting the development and review of L1 a/b/c processors and the performance monitoring facility. In 2024, he was also appointed as the Engineering Support Service (ESS) Manager for the area supporting all ESA Earth Explorers PDGS developments in European Space Research Institute (ESRIN), Frascati, Italy.

Adriano Carbone received the Ph.D. degree in electronics from the University of Rome "Sapienza," Rome, Italy, in 2006.

He has been a Research Fellow at Italian Space Agency (ASI), Matera, Italy, and has worked in space industry before moving to ESA/ESTEC, Noordwijk, The Netherlands, in 2009, initially as part of the Sentinel-1 team. After the launch and commissioning of S1-A satellite, he moved to the BIOMASS project with the role of an Instrument Principal Engineer with a focus on the development and verification of the flight HW and SW and system engineering. Currently, he is the Instrument Development Coordinator for the Copernicus Radar Observing System for Europe at L-band (ROSE-L) mission.

Nuno Carvalhais received the Ph.D. degree in environmental sciences and engineering from the Faculty of Sciences and Technology, NOVA University of Lisbon, Caparica, Portugal, in 2010.

He is a Senior Scientist and the Group Leader of the Model–Data Integration Group, Department of Biogeochemical Integration, Max Planck Institute for Biogeochemistry (MPI-BGC), Jena, Germany. His research integrates Earth observation with theory and modeling, including hybrid modeling, to quantify terrestrial ecosystem dynamics and carbon–water cycle variability and fluxes. He is involved in ESA's BIOMASS Mission Advisory Group and leads the BIOMASS Project Office Germany.

Jérôme Chave, photograph and biography not available at the time of publication.

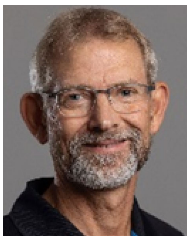

Jørgen Dall (Member, IEEE) received the M.Sc. and Ph.D. degrees from the Technical University of Denmark, Kongens Lyngby, Denmark, in 1984 and 1988, respectively.

He is currently a Professor in microwave remote sensing systems with the Technical University of Denmark. He led the development of a dedicated real-time SAR processor for the first Danish airborne SAR, EMISAR, and he led the development of ESA's airborne SAR and ice-sounding radar, POLARIS. Most recently, he led the development of a ground-based X-band MIMO radar. Since 1990, he has been in charge of the EMISAR and POLARIS campaigns that have primarily been flown in Denmark, Greenland, and Antarctica. His research interests include ice sheet mapping with InSAR, Pol-InSAR, and TomoSAR, and radar ice sounding. Since 2009, he has been a member of ESA's BIOMASS mission advisory group.

Michael Fehringer received the master's and Ph.D. degrees from Vienna University of Technology, Vienna, Austria.

He worked as a Research Fellow at ESA, Noordwijk, The Netherlands, from 1987 to 1989 before joining Austrian Research Centre Seibersdorf, Seibersdorf, Austria, where he developed and built scientific instruments for space science satellites. In 2000, he joined ESA again working as a System Engineer and later a System Manager of the GOCE mission. In 2014, he was appointed as a Project Manager for the Biomass mission.

Antonio Leanza, photograph and biography not available at the time of publication.

Thuy Le Toan received the Ph.D. degree in atomic and nuclear physics from the University of Toulouse, Toulouse, France, in 1973.

She led the Biomass Group, CESBIO, a research laboratory affiliated with CNRS, CNES, INRA, IRD, and the University of Toulouse. Her research focuses on radar remote sensing of land surfaces. She has conducted experimental and modeling work within the framework of numerous projects for CNES, ESA, NASA, JAXA, and European Union. These projects aim to understand the physical content of the SAR signal as a function of the biophysical properties of vegetation in forests and cultivated lands, to define the sensors and methods to be developed for applications. Interested in the role of forests in climate change and the global carbon balance, she proposed the P-band SAR Biomass mission in 2005, along with a group of international scientists. She is the author of 382 peer-reviewed journal articles and book chapters.

Dr. Le Toan was a member of the JAXA Kyoto and Carbon Initiatives and is currently the Co-Lead of the Asia-Rice Initiative. For nearly 20 years, she co-chaired the Biomass Mission Advisory Group. She has served on numerous national and international Earth observation advisory committees.

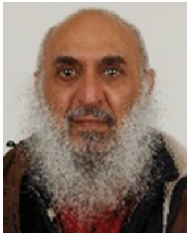

Maktar Malik received the Ph.D. degree from the University of Kent, Canterbury, U.K., in 1996.

From 2000 to 2021, he worked in the Galileo GNSS program holding a number of positions in Space Segment. He is Giove B Payload Systems Manager at EADS Astrium (also known as ADS), Portsmouth, U.K. He is also a Navigation Payload Principal Engineer for Giove A, B, and 4 IOV spacecraft at ESA, Noordwijk, The Netherlands. He is a Spacecraft Systems Principal Engineer responsible for leading Galileo 2nd Generation satellite system activities, managing the parallel Phase A/B1 contracts with ADS, TASI, and OHB. He joined Biomass in 2021 and is currently the BCT Lead responsible for BCT transponder and IOC phase commissioning lead, coordinating all IOC activities and tasks for the multidisciplinary teams.

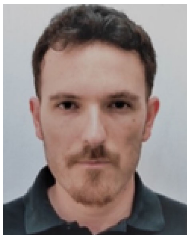

Antonio Novelli received the Ph.D. degree from the Politecnico di Bari, Bari, Italy, in 2017.

He has held positions as a university researcher and a teacher in geomatics and remote sensing, a senior researcher in geospatial applications for renewable energies, and a senior technical specialist for high-level remote sensing data applications. He also worked as a BIOMASS Level 2 PDGS Engineer, supporting the BIOMASS PDGS development and operational processors' review. Notable achievements include contributing to successful EU tenders and proposals, holding Italian National Academic qualification as an Associate Professor in geomatics. He has authored or co-authored over 50 scientific publications, including journal articles, conference proceedings, and reports.

Philippe Paillou received the Ph.D. degree from the University of Strasbourg, Strasbourg, France, in 1992.

Since 1994, he has been a Professor at the University of Bordeaux, Bordeaux, France. He conducts comparative studies between arid areas on Earth (Sahara and Central Asia) and planetary surfaces (Venus, Mars, and Titan), using low-frequency SAR systems for subsurface moisture detection and geology mapping. His most significant research results concern the discovery of impact craters in Libya and of a large crater field in Egypt, the discovery of major paleo rivers in Libya and Mauritania, participation to the discovery of methane lakes on Titan, and the revealing of a radar phase signature to map subsurface moisture and soil salinity. He participated in several solar system exploration and Earth observation missions: ALOS/PALSAR and ALOS-2 (JAXA), CASSINI-HUYGENS (NASA/JPL), EXOMARS (ESA), and MARS2020 (NASA/CNES).

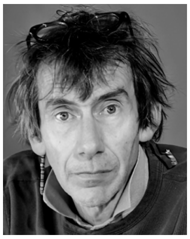

Kostas P. Papathanassiou (Fellow, IEEE) received the Dipl.-Ing and Dr. degrees from the Technical University of Graz, Graz, Austria, in 1994 and 1999, respectively.

From 1992 to 1994, he was with the Institute for Digital Image Processing (DIBAG) of Joanneum Research, Graz. From 1995 to 1999, he worked at the Microwaves and Radar Institute (HR), German Aerospace Center (DLR), Weßling, Germany. From 1999 to 2000, he was an EU Postdoctoral Fellow with Applied Electromagnetics (AEL), St. Andrews, U.K. Since October 2000, he has been with HR, DLR, where he is currently a Senior Scientist leading the Information Retrieval Research Group. His main research interests are in polarimetric and interferometric processing and calibration techniques, polarimetric SAR interferometry, and the quantitative parameter estimation from SAR data, as well as in SAR mission design and SAR mission performance analysis. He is a member of DLR's TanDEM-X and Tandem-L science teams, JAXA's ALOS-PalSAR Cal-Val teams, ESA's BIOMASS Mission Advisory Group, and JAXA's Carbon and Kyoto Initiative and NASA's GEDI Mission Science Team. He has more than 80 peer-reviewed articles in international journals and more than 400 contributions in international conferences and workshops.

Dr. Papathanassiou was awarded with the IEEE GRSS IGARSS Symposium Prize Paper Award in 1998, the Best Paper Award of the European SAR Conference (EUSAR) in 2002, and the IEEE GRSS J-STARS Paper Award in 2019. He received the DLR Science Award in 2002 and 2020, the DLR's Senior Scientist Award in 2011, the IEEE Fellow Award in 2015, and the DLR's Otto Lilienthal Award in 2020.

Janice Patterson, photograph and biography not available at the time of publication.

Muriel Pinheiro received the B.S. degree in electronic engineering and the M.S. degree in telecommunications from the Aeronautical Technological Institute, São José dos Campos, Brazil, in 2009 and 2010, respectively, and the Dr-Ing. degree (honors) from Karlsruhe Institute of Technology, Karlsruhe, Germany, in 2016.

From 2009 to 2010, she was at BRADAR, Sao Jose dos Campos, Brazil, working with the development of calibration algorithms for airborne SAR interferometry. From 2011 to 2021, she was at the Microwaves and Radar Institute, German Aerospace Center (DLR), Weßling, Germany, where she was a member of the Multimodal Algorithms Group. Her research topics included signal and image processing, advanced techniques for SAR image formation, end-to-end SAR simulation, SAR interferometry, high-resolution DEM generation, and persistent scatterer interferometry. In 2021, she joined European Space Agency (ESA), Frascati, Italy, as a Calibration and Validation Engineer for SAR missions, with special focus on the quality assurance of Sentinel-1 products and development of processors and algorithms for the upcoming BIOMASS and ROSEL missions.

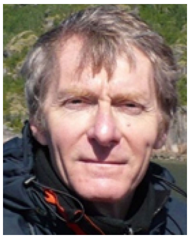

Shaun Quegan is a Professor with the School of Mathematical and Physical Sciences, The University of Sheffield, Sheffield, U.K., and a member of the National Centre for Earth Observation, Sheffield. His research over the last 35 years has been mainly concerned with using satellite data and ecosystem models to clarify the role of the land surface, and especially forests, in the Earth's carbon cycle and climate, and he directed the NERC Centre of Excellence in Terrestrial Carbon Dynamics. He is a Joint Proposer and a Lead Scientist of European Space Agency BIOMASS mission, launching in April 2025, which will measure forest biomass, height, and disturbance worldwide using highly innovative radar technology. He has served on numerous national and international committees advising on climate and Earth observation by satellites and has written two books (on radar and synthetic aperture radar), together with 160 journal articles.

Markus Reichstein received the Ph.D. degree from the University of Bayreuth, Bayreuth, Germany, in 2001. He studied landscape ecology at the University of Münster, Münster, Germany.

He is the Director of the Department of Biogeochemical Integration, Max Planck Institute for Biogeochemistry, Jena, Germany, and a Professor of global geoecology at Friedrich Schiller University Jena, Jena. His research focuses on understanding and predicting ecosystem responses and feedbacks to climate variability and extremes from an Earth system perspective, linking vegetation, soils, and coupled carbon, water, and nutrient cycles, and combining observations, Earth observation, model–data integration, and machine learning. He is a Founding Co-Director of the Michael Stifel Center Jena for Data-Driven and Simulation Science and a Founding Co-Director of the ELLIS program "Machine Learning for Earth and Climate Science" and the ELLIS Unit Jena, Jena.

Dr. Reichstein was elected as a member of German National Academy of Sciences Leopoldina and an AGU Fellow in 2025.

Björn Rommen received the M.S. degree in electrical engineering from Delft University of Technology, Delft, The Netherlands, in 1999.

Since 1999, he has been working in the field of Earth observation at the Research and Technology Centre, European Space Agency (ESA), Noordwijk, The Netherlands. He is currently a Mission Scientist for ESA's Earth Explorer 7 Biomass and Earth Explorer 10 Harmony missions. His research interests include a wide range within the domain of active microwave remote sensing—involving work at both microwave instrument conceptual level and leading research and development activities investigating wave interaction with the earth's surface (including bio/geophysical parameter retrieval) and atmosphere—which, to a large extent, has been driven by synthetic aperture radar (SAR) missions in preparation at ESA. He has been involved in the Sentinel-1A, -1B, and -1C prelaunch and postlaunch activities, including the commissioning phases covering overall SAR in-orbit performance and system calibration activities. His research interests include electromagnetics theory, computational electromagnetics, and radar remote sensing.

Sassan Saatchi, photograph and biography not available at the time of publication.

Herman H. Shugart is the W. W. Corcoran Professor (Emeritus) with the Department of Environmental Sciences, University of Virginia, Charlottesville, VA, USA. He has served as the major advisor to 26 completed M.Sc. students, 56 completed Ph.D. students, and 22 postdoctoral associates. He is the author or co-author of 502 publications, including six books, seven edited books (plus seven additional reprintings of books and edited books), 96 book chapters, and 213 articles in peer-reviewed journals on forests mostly on ecological modeling and global ecology.

Tristan Simon, photograph and biography not available at the time of publication.

Stefano Tebaldini (Senior Member, IEEE) received the M.Sc. degree in telecommunication engineering and the Ph.D. degree from Politecnico di Milano, Milan, Italy, in 2005 and 2009, respectively.

Since 2005, he has been with the Digital Signal Processing Research Group, Politecnico di Milano, where he has held an associate professor position at the Dipartimento di Elettronica, Informazione e Bioingegneria since 2018. He is a member of the BIOMASS Mission Advisory Group at ESA, tasked with providing scientific and technical advice on the BIOMASS Mission. His research is mostly focused on imaging radars. His research activities include spaceborne, airborne, automotive, and ground-based synthetic aperture radar (SAR) processing, multistatic and distributed radars processing, calibration, accurate platform localization, synchronization recovery, and ionospheric correction. He has authored over 60 articles published in international peer-reviewed journals.

Dr. Tebaldini's work on FDM MIMO SAR received the Best Paper Award from EuSAR 2024.

Lars M. H. Ulander (Fellow, IEEE) received the M.Sc. degree in engineering physics and the Ph.D. degree in electrical and computer engineering from the Chalmers University of Technology, Gothenburg, Sweden, in 1985 and 1991, respectively.

He worked at Swedish Defence Research Agency (FOI), Linköping, Sweden, from 1995 to 2026 with the airborne CARABAS and LORA SAR systems. He has been a Full Professor in radar remote sensing at the Chalmers University of Technology since 2014. His research areas include synthetic aperture radar (SAR), radar imaging, signal processing, electromagnetic scattering, and remote sensing applications. He is the author or co-author of over 400 professional publications, of which more than 90 are in peer-reviewed scientific journals.

Dr. Ulander received the Thulin Medal in silver from Swedish Society of Aeronautics and Astronautics for pioneering research in VHF- and UHF-band SAR.

Antonio Valentino received the M.S. degree in electronic engineering from the Politecnico di Torino, Turin, Italy, in 2000.

Since 2001, he has been working on synthetic aperture radar (SAR) processing, calibration, and applications, and he has worked on important international SAR missions, including COSMO-SkyMed, Sentinel-1, SAOCOM, BIOMASS, and the upcoming ROSE-L. He is currently a Contractor with European Space Research Institute (ESRIN), European Space Agency (ESA), Frascati, Italy, covering the role of SAR data quality specialist.

Philip Willemsen received the Diploma and Ph.D. degrees in physics from Rheinische Friedrich-Wilhelms-Universität Bonn, Bonn, Germany, in 2001 and 2004, respectively.

He was a Systems Engineer and a Project Manager of satellite and space technology demonstration projects with German Aerospace Center, Bonn. He joined European Space Agency, Noordwijk, The Netherlands, in 2011, where he has led the design and development of systems from concept phases to flight hardware manufacturing and launch. From 2014 to 2020, he was the Principal Instrument Engineer of the Meteosat Third Generation, MTG Lightning Imager. Since 2020, he has been the Biomass System and Mission Performance Manager.

Mathew Williams received the B.A. degree from the University of Oxford, Oxford, U.K., and the Ph.D. degree from the University of East Anglia, Norwich, U.K., in 1994.

He leads the Global Change Ecology Laboratory, School of Geosciences, The University of Edinburgh, Edinburgh, U.K. Over the past 25 years, his research has focused on studying the carbon cycle of terrestrial ecosystems, including Arctic tundra, the Amazon rainforest and African savannas, and U.K. landscapes under management. This research has informed society both on how ecosystems will respond to climate change and how ecosystem responses will change the global carbon cycle. His research currently focuses on combining environmental simulation models with field data and satellite observations to understand the flows of carbon, energy, and water across natural and managed landscapes. He explores the climate sensitivity of forests and tundra, the effect of fires and harvests on forest biomass, monitoring of U.K. and global greenhouse gas balances from space and tall towers, and forecasting climate and management impacts on ecosystems.

Prof. Williams received the Royal Society Wolfson Merit Award in 2014. He is a Principal Investigator with the U.K. National Centre for Earth Observation and is an advisor to European Space Agency. He has served on the Science Board for the UKRI Natural Environment Research Council. He is currently seconded to Scottish Government as a Chief Scientific Adviser for Environment, Natural Resources, and Agriculture.